Proc. NIPR Symp. Upper Atmos. Phys., **11**, 106–120, 1998

QUASI-STEADY PRODUCTION OF REGION 1 AND REGION 2 FIELD-ALIGNED CURRENTS

Takashi YAMAMOTO[1] and Shoshi INOUE[2]

[1]*University of Tokyo, 3–1, Hongo 3-chome, Bunkyo-ku, Tokyo 113*
[2]*Aichi College of Technology, Gamagohri 443*

Abstract: Quasi-steady production of the hot plasma torus (HPT) in the magnetosphere and simultaneous generation of the region 1 and region 2 field-aligned currents (FACs) are numerically simulated for the case of southward interplanetary magnetic field. The magnetosphere-ionosphere coupling is treated in the two-dimensional electrostatic simulation model, and particularly incorporated are effects of the following processes: 1) nonadiabatic acceleration of ions incident on the tail plasma sheet (including particle acceleration at the magnetic reconnection), 2) plasma escape, along the open field lines, to the interplanetary space, and 3) anomalous cross-field diffusion of plasma particles. Under the condition that the open-closed boundary is distorted by the two-cell convection, the region 1 FAC (as well as the region 2 current) is steadily generated by a pressure-gradient mechanism. (Convection-distortion here means that the center of the circle fitted to the open-closed boundary (projected onto the ionospheric plane) is shifted antisunward so that this center is positioned at a latitude (on the midnight meridian) lower than that of the (averaged) ionospheric projection of the path of a magnetically drifting particle in the magnetosphere.) The simulations show that the HPT can be maintained as long as continual particle injection and energization take place, which implies that the primary energy source for the HPT and FACs is the particles nonadiabatically accelerated near the nightside injection boundary.

1. Introduction

Since the characteristics of large-scale field-aligned currents (FACs) were statistically summarized by IIJIMA and POTEMRA (1976, 1978), there have been a number of theoretical works on the FAC generation (for reviews, see SISCOE and MAYNARD (1991) and YAMAMOTO *et al.* (1996)). Most of the previous theories associated the generation of region 1 current with the boundary layer processes such as the magnetic reconnection (DUNGEY, 1961) and the viscous interaction (AXFORD and HINES, 1961; SONNERUP, 1980). However, the recent data analysis of the magnetic field perturbation and the particle flux measured from the Defense Meteorological Satellite Program (DMSP) F7 satellite (IIJIMA *et al.*, 1991; WATANABE and IIJIMA, 1993) has shown that on the nightside the region 1 FAC (as well as the region 2 current) coexists with enhanced precipitation of hot ($\gtrsim$1 keV) particles in the magnetically closed region. In our paper the combined system of the region 1 and region 2 FACs is referred to as the paired region 1/region 2 FACs (which exclude the region 1 current connected to the low-latitude boundary layer (LLBL)). The coexisting hot particle population in the magnetosphere is called the hot plasma torus (HPT), which can be regarded as the source of the paired region 1/region 2 FACs. Specifically, the HPT is the combined regions of the boundary plasma sheet (BPS) and the central plasma sheet (CPS).

Based on the correlation between the HPT and the paired region 1/region 2 FACs, YAMAMOTO and OZAKI (1993) and YAMAMOTO *et al.* (1996) studied a theoretical model that these FACs can be generated as a result of "natural distortion" of the HPT under the influence of the two-cell convection: owing to the distortion, the pressure gradient in the HPT gains a component parallel to the magnetic drift so that the particle magnetic drifts induce the polarization of the HPT with the polarity consistent with the observed pattern of the region 1/region 2 FACs. (The magnetic drift means the gradient B drift plus the curvature drift for charged particles.) However, their model assumes a priori the presence of the HPT.

The purpose of the present paper is to numerically study the processes for quasi-steady production of the HPT in the magnetosphere and simultaneous generation of the paired region 1/region 2 FACs. We consider the case in which the interplanetary magnetic field (IMF) B_z is negative so that the open-closed boundary is clearly defined and it is distorted by the two-cell convection. Convection-distortion here is defined as follows: When the path of a magnetically drifting particle as well as the open-closed boundary on the nightside (as projected onto the ionospheric plane) are fitted to circles, the center of the open-closed boundary circle is shifted to a latitude lower than that of the magnetic drift circle, by the effect of a two-cell convection. The (distorted) distribution of the open-closed boundary relative to the magnetic drift direction was first inferred by HRUŠKA (1986) from particle observations of the ISEE 1 satellite, although he did not discuss the cause of the distortion.

There are three fundamental processes which are important for the HPT formation: 1) nonadiabatic acceleration of ions incident on the tail current sheet (including particle acceleration in the magnetic reconnection), 2) plasma escape, along the open field lines, to the interplanetary space, and 3) anomalous cross-field diffusion of plasma particles. Incorporating the effects of these processes, our two-dimensional simulations show that the HPT can be maintained as long as continual particle injection and energization take place. Renewal of particles in the HPT proceeds in the presence of the two-cell convection which is created by polarization of the HPT, *i.e.*, generation of the region 1/region 2 FACs. Due to the azimuthal pressure gradient appearing on the convection-distorted HPT, the region 1/region 2 FACs are produced, approximately, in the region of $\partial N/\partial x < 0$ and $\partial N/\partial x > 0$, respectively, where N is the flux tube content of the HPT particles, and x is the latitudinal coordinate on the ionosphere and the positive direction is poleward. A "natural" latitudinal N-profile of the HPT with a single peak inside it can be maintained by the aid of both particle escape (in the open region) away from the Earth and anomalous cross-field diffusion.

2. Modeling

In this section we briefly describe a simulation model for the simultaneous production of the HPT and the paired region 1/region 2 FACs. For treating only the quasi-steady (time scale longer than several minutes) currents we adopt the electrostatic model which neglects the effect of the Alfvén wave transmission in the magnetosphere. As is studied by YAMAMOTO *et al.* (1996), we are allowed to consider only the HPT particles with keV energies as the dominant source for the paired region 1/region 2 FACs. In the present simulations the drift approximation can be used for the perpendicular motions of particles because the temporal and spatial scales of the large-scale currents are much greater than the ion cyclotron period and radius. As is discussed by YAMAMOTO *et al.* (1996), the inertia drift can be ignored.

The followings are the main assumptions made in our two-dimensional simulations for the magnetosphere-ionosphere coupling.

(1) A singly ionized hydrogen plasma is considered. (Each particle species is treated as a fluid.) The pressure of each particle species is isotropic and uniform along the field lines.

(2) The magnetic field lines are equipotential. The ambient field on the ionosphere is perpendicular to the ionospheric plane and its strength B_i is uniform.

(3) The precipitation of the ions as well as the supply of ions from the ionosphere are ignored.

(4) Immediately after injection into the closed region, the protons (near the open-closed boundary) are nonadiabatically accelerated up to about 3 keV and subsequently they are adiabatically energized, so that their average energy, W^p, is proportional to $R_B^{-2/3}$ where R_B is the volume of a flux tube with one unit of magnetic flux. The electron average energy W^e is also proportional to $R_B^{-2/3}$. Before injection the particles have no kinetic energy. (Nonadiabatic acceleration process itself is not self-consistently included.)

(5) The ionospheric projection of a magnetic drift path is a circle with the center near the magnetic pole. The average magnetic drift speed ($\bar{V}_{m,i}$) projected onto the ionospheric plane (for each particle species) is constant. For the HPT protons and electrons, $\bar{V}_{m,i}$ is taken as 0.16 km/s and 0.08 km/s, respectively.

(6) The ionospheric (height-integrated) conductivities are assumed simply to be uniform. The height-integrated Pedersen conductivity is taken as 4 mho.

(7) The open-closed boundary is distorted by the (two-cell) convection in the sense that the center of the circle fitted to the open-closed boundary is positioned, on the midnight meridian, at a latitude lower (2.8 degrees) than that of the circle fitted to the magnetic drift path.

(8) The HPT protons are subject to the (anomalous) cross-field diffusion. (Wave-particle interaction responsible for the anomalous diffusion is not included.)

(9) The HPT particles existing out of the closed region escape to the interplanetary space with a characteristic time of several minutes. (The specific description of particle escape will be given later.)

In general, the conservation of particles of species j (**p**roton or **e**lectron) in a flux tube can be expressed in terms of two-dimensional variables defined on the ionospheric plane

$$\frac{\partial}{\partial t} N^j + \mathrm{div}_i \Gamma^j = Q^j - L^j, \qquad (1)$$

where div_i is operated on the ionospheric plane. In the above expression N^j is the number of particles in a flux tube with unit (ionospheric) cross section:

$$N^j = \int_{s_i}^{s_e} n^j \frac{B_i}{B(s)} \mathrm{d}s, \tag{2}$$

where s is the field-aligned distance, s_e and s_i are at the equator and the ionospheric height; $B(s)$ and B_i are the magnetic field intensities at the distances s and s_i, respectively, n^j is the number density of the species j; the particle influx Q^j and outflux L^j represent supply from and precipitation into the ionosphere, respectively; the lateral particle flux is defined as

$$\Gamma^j = \int_{s_i}^{s_e} n^j (V_{E,i}(s) + V^j_{m,i}(s)) \frac{B_i}{B(s)} \mathrm{d}s, \tag{3}$$

where $V_{E,i}(s)$ and $V^j_{m,i}(s)$ are the ionospheric projections of the electric and magnetic drift (gradient B drift plus curvature drift) velocities, $V_E(s)$ and $V^j_m(s)$, of the j species fluid. From assumptions 1 and 2, the number density n^j is found to be uniform along the field lines. On the equipotential field lines, $V_{E,i}(s)$ at any distance s is identical to $V_E(s_i)$, *i.e.*, the electric drift velocity on the ionospheric plane. (Hereafter $V_E(s_i)$ is simply denoted by $V_{E,i}$.) The flux Γ^j in eq. (3) is then written as

$$\Gamma^j = N^j (V_{E,i} + \bar{V}^j_{m,i}),$$

using the average magnetic drift velocity $\bar{V}^j_{m,i}$ defined as

$$\bar{V}^j_{m,i} = \frac{1}{R_B} \int_{s_i}^{s_e} V^j_{m,i}(s) \frac{1}{B(s)} \mathrm{d}s = W^j \bar{\nu}^j_{m,i} \text{ and } R_B = \int_{s_i}^{s_e} \frac{1}{B(s)} \mathrm{d}s, \tag{4}$$

where W^j is the average energy of the j species fluid, and $\bar{\nu}^j_{m,i}$ is the averaged value of the ionospheric projection of the magnetic drift velocity per unit energy. Note that the integration in eq. (4) is equivalent to averaging over all the j species particles in a magnetic flux tube volume when the density distribution is uniform along the field lines as assumed above. The particle conservation is now written as

$$\frac{\partial N^j}{\partial t} + \mathrm{div}_i\{N^j (V_{E,i} + \bar{V}^j_{m,i})\} = Q^j - L^j. \tag{5}$$

For the HPT protons both Q^p and L^p are assumed negligible (assumption 3). The total electron flux of $e(Q^e - L^e)$ is considered to be given by the field-aligned current density $J_{\parallel i}$ at the ionospheric height.

On the basis of the particle conservation law (5), we suppose the population of "virtual particles" confined on the ionospheric plane as representing the cross-field dynamics of the HPT particles in the magnetosphere. The positions of individual virtual particles are given by the ionospheric projections of the HPT particles. Taking the projections of all the HPT particles, the "surface" number density of the virtual particles can be taken as N^j. In conformity with eq. (5), we can assume that the virtual particles are moved by the electric drift due to the ionospheric field as well as by the magnetic drift of the velocities $\bar{V}^j_{m,i}$ defined in eq. (4).

Under assumption (4) that the average energies, W^p and W^e, for the HPT protons and electrons are proportional to $R_B^{-2/3}$, the FAC density, $J_{\parallel i}$, at the ionospheric height can be expressed in terms of the HPT flux tube content $N (= N^p \cong N^e)$ (see YAMAMOTO *et al.*, 1996):

$$J_{\| i} = (\bar{V}^{p}_{m,i} - \bar{V}^{e}_{m,i}) \cdot \nabla_i N, \tag{6}$$

where e is the electronic charge and ∇_i denotes the gradient on the ionospheric plane. The positive value of $J_{\| i}$ is for the FAC flowing away from the ionosphere, *i.e.*, the upward FAC. In eq. (4) the product of $W^j\,|\bar{\nu}_{m,i}|$ does not so much change with latitude as either W^j or $|\bar{\nu}_{m,i}|$ because the increase of W^j (with decreasing latitude) is partially cancelled out by the decrease of $|\bar{\nu}_{m,i}|$. In the present model, for simplicity the magnetic drift speeds, $|\bar{V}^{p}_{m,i}| = W^p\,|\bar{\nu}_{m,i}|$ and $|\bar{V}^{e}_{m,i}| = W^e\,|\bar{\nu}_{m,i}|$ are assumed constant (assumption 5). Note that the effect of the adiabatic particle acceleration on the FAC generation is implicitly included in this assumption. Also, note that as a first approximation, the particle acceleration/deceleration by the (steady) electrostatic field is equivalent to the energy variation such that W is proportional to $R_B^{-2/3}$.

Using the FAC density $J_{\| i}$, the electrostatic potential arising from the polarized HPT is calculated from the ionospheric current continuity

$$J_{\| i} = -\Sigma_p \mathrm{div}_i \boldsymbol{E}_i, \tag{7}$$

where Σ_P is the height-integrated Pedersen conductivity and $\boldsymbol{E}_i$ is the ionospheric electric field. Note that divergence of the Hall current is negligible for the uniform height-integrated conductivities (assumption 6). In the simulations Σ_P is taken as 4 mho. The ionospheric potential is solved under the boundary condition that the potential vanishes at a latitude of 62°. Note that the ionospheric potential distribution is essentially the same as the magnetospheric potential distribution, under the assumption of equipotential field lines. The $E\times B$ drift velocity of the virtual particles is calculated assuming that the magnetic field strength on the ionosphere is 6×10^4 nT.

Assumption (7) is supported by the following observational facts: MENG *et al.* (1977) examined DMSP auroral photographs of bright extended quiet arcs and found that an off center circle in corrected geomagnetic latitude-MLT coordinates (HULTQVIST, 1958a, b; HAKURA, 1965; GUSTAFSSON, 1970) is the best fit to these quiet arcs. The centers of the auroral circles were found to be concentrated within a circular areas of 3° radius centered at ~4.2° away from the geomagnetic pole along the 0010 MLT (nearly midnight) meridian. Since most of bright discrete arcs extending over extensive local time hours delineate the poleward boundary of the auroral oval which may be regarded as the open-closed boundary, the center of the open-closed boundary circle is likely to be located at about 85.8° in corrected geomagnetic latitude on the nearly midnight meridian. On the other hand, MCDIARMID *et al.* (1975) obtained the average intensity contours for electrons with energies greater than 210 keV and pitch angles ranging from 45° to 135°, using the ISIS 2 satellite observations at an altitude of 1400 km during the relatively quiet ($K_p \leq 3o$) periods. As is discussed by YAMAMOTO *et al.* (1996), the intensity contours for such energetic electrons may be regarded as the average magnetic drift path projected onto the ionospheric plane, and the circle fitted to the average intensity contour passing near the poleward edge of the nightside auroral oval has a center at ~88.5° in invariant latitude (MCILWAIN, 1961) on the midnight meridian. Hence the center of the magnetic drift circle is likely to be positioned at ~88.5° in invariant latitude on the midnight meridian. If this position is expressed in terms of corrected geomagnetic latitude-MLT coordinates, the difference in latitude is presumed to be less than about 1 degree. Therefore, assumption (7) may be reasonable.

LYONS and SPEISER (1982) have shown that ions incident on the tail current sheet can be nonadiabatically accelerated due to the dawn to dusk electric field; the characteristic particle energy is increased from several hundred electron volts to a few kilo electron volts (see Figs. 2, 3, 9 and 10 of their paper). The velocity distribution of accelerated ions which results from the current sheet acceleration was also shown to be consistent with the observations at the outer edge of the plasma sheet. Since the ion beams are frequently observed, by the midaltitude Akebono satellite, in a relatively wide range of 20–04 MLT (SAITO *et al.*, 1992), the current sheet acceleration in the tail may be regarded as an important energy source of plasma sheet ions. Similar ion acceleration can occur in the reconnection process. According to the numerical calculation of test particle trajectories in developing reconnection fields (SATO *et al.*, 1982), ions can be accelerated near the neutral line to 1–200 keV, depending on how close they reach the neutral line after injection. Thus, in our simulations the kinetic energy of the HPT is assumed to be provided by the nonadiabatic ion acceleration in the tail and the subsequent adiabatic heating of the particles (assumption 4).

YAMAMOTO *et al.* (1997b) have shown that owing to the low-frequency wave turbulence such as the broadband electrostatic noise and the Alfvén wave noise, the anomalous cross-field diffusion coefficient averaged over the flux tube, for the HPT protons, is likely to reach a significant fraction of the Bohm rate at least in the disturbed periods. Basically, the wave turbulence is generated at the expense of particle kinetic energy. Then, roughly speaking, the anomalous diffusion coefficient is proportional to the (HPT) flux tube energy content, *i.e.*, $(W^p+W^e)\,N$. In our simulations we assume that the proton diffusion coefficient reaches, in the middle (in latitude) of the HPT domain, about 20% of the Bohm rate (*i.e.*, $(2W^p/3)/16eB$) for protons energized to $W^p=6$ keV, and that it is decreased toward the HPT boundaries and vanishes on them. Due to a difference in the diffusion rate between ions and electrons, FACs can be produced as studied by YAMAMOTO *et al.* (1997b). In the present model, however, the diffusion-induced FACs are not included.

The high-latitude side of the HPT, where $\partial N/\partial x$ is negative, is unstable against the interchange instability, due to the oppositely directed magnetic drifts of the HPT protons and electrons. As is studied by YAMAMOTO *et al.* (1997c), however, the whole structure of the HPT can be maintained in the closed region by the effects of magnetic drift reversal across the open-closed boundary and/or the outward pressure gradient in the LLBL, although interchange fluctuations will appear on the high-latitude side of the HPT. In case that the majority of the HPT particles are convected to inner magnetic shells as is supposed to occur in the recovery phase of a substorm (for precise condition, see YAMAMOTO *et al.*, 1997c), the interchange instability can fully be developed with a result consistent with the formation of auroral omega bands and torch-like structures (YAMAMOTO *et al.*, 1993, 1997d). To focus the present analysis on the global generation of FACs, we suppress the growth of these fluctuations by modifying the potential distribution resulting from the region 1 FAC: In calculating the potential the pattern of the relative FAC density is replaced by that of the initial region 1 FAC and the absolute current density is given so that the total potential drop resulting from the modified region 1 FAC is the same as that calculated from the instantaneous distribution (in region 1 zone) of the HPT particles. (As for the large-scale structure, the difference between the modified and instantaneous potential distributions turns out to be small.)

The numerical simulations are performed in the (ionospheric) polar region at invariant latitudes greater than 62°, by using a particle-in-cell code (*e.g.*, OKUDA, 1985). This circular simulation domain is covered with 128×512 grid meshes in polar coordinate (r, ϕ). The magnetic local time increases in the counterclockwise direction and the midnight meridian is set at the radial axis pointing downward. The grid spacing Δr is then about 24 km, and $r\Delta\phi$ is, for example, about 27 km at an (invariant) latitude of 70°. In the two-dimensional guiding center model the grid spacing is not required to be less than the ion Larmor radius nor the Debye length, and the time step is not required to be less than the ion cyclotron period. The guiding center positions of (virtual) particles are advanced by using the predictor-corrector method (LEE and OKUDA, 1978). The time step Δt is taken small enough to satisfy the Courant condition of $V_{max}\Delta t < \Delta r$ (or $r\Delta\phi$), where V_{max} is the maximum particle speed. The results to be presented are from runs using a time step of $\Delta t = 10.2$ s. About 90000 particles are used for the HPT protons. (As is discussed by YAMAMOTO *et al.* (1997a), because of charge neutrality condition and assumption (3) we are allowed to follow only the dynamics of the HPT protons as representing the whole HPT dynamics in a plane perpendicular to the magnetic field.) To create a nonuniform density, they have different weights in charge q and mass M, but the ratio of M/q is fixed. There is no need for loading the background cold particles (in the magnetosphere), because the charge separation (as is responsible for generation of quasi-steady large-scale currents) does not take place in this particle population.

3. Initial Conditions and Results

The initial distribution of the (preexisting) HPT particles is shown in Fig. 1. Here indicated is the number density n_i of the particles, which is defined as $n_i = N/(R_B B_i)_0$ where $(R_B B_i)_0$ is the value of $R_B B_i$ on the R_B-equicontour passing a point at 67.8° latitude on the midnight meridian. (Note that the R_B-equicontour is identical to the average magnetic drift path (YAMAMOTO *et al.*, 1996.) Actually, $(R_B B_i)_0$ is taken as 1.32×10^7 km, which is the value of $(R_B B_i)_0$ for the dipole field line at $L = 7\ R_E$. Note that the density n_i is proportional to the flux tube content N, while n_i, only at that R_B-contour, is equal to the HPT (local) density in the magnetosphere. Figure 1a indicates the region where the HPT particles exist initially; this region is encompassed by two eccentric circles centered on the midnight meridian. Figure 1b shows the latitudinal profile $n_i(x)$, as an example, at 20 hours in magnetic local time (MLT), where the x direction is perpendicular to the magnetic drift path and the HPT width here is about 300 km. (To save the time for computation, the latitudinal width of the HPT is taken to be smaller than that of the FAC region identified from the observations.) In our model the poleward boundary of the initial HPT coincides with the open-closed boundary. Just outside of the closed region, plasma particles with $n_i = 4$ cm^{-3} are steadily supplied from a particle reservoir for injection. The actual injection boundary is natural-

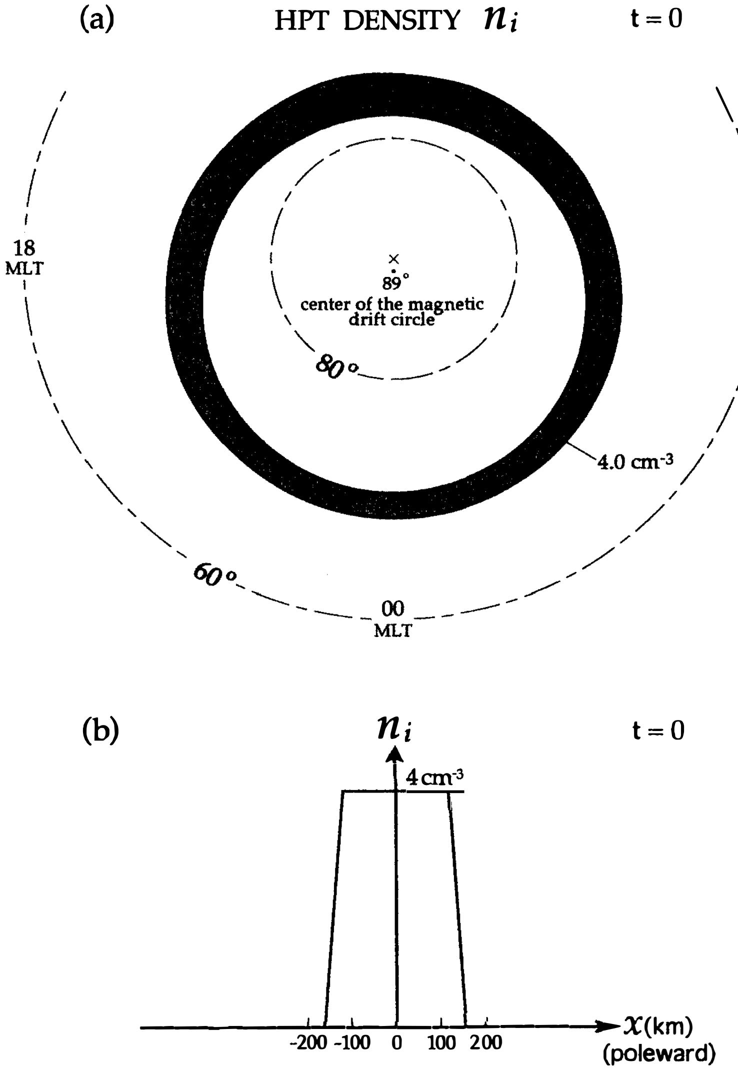

Fig. 1. *Initial distribution of the (preexisting) HPT particles for run 1. (a) Region of the HPT projected onto the ionospheric plane and (b) latitudinal profile of the number density $n_i(x)$ (defined in text) at 20 MLT.*

ly determined as a part of the open-closed boundary on which the $E \times B$ flow has an inward (toward lower latitude) component. (The injection boundary defined for the initial potential distribution is indicated in Fig. 3.) Since the centers of the poleward and equatorward HPT boundary circles are assumed to be (on the midnight meridian) at latitudes lower than that of the magnetic drift circle, polarization occurs, on the HPT, due to oppositely directing magnetic drifts of the HPT electrons and protons: the poleward and equatorward boundaries on the evening-side are negatively and positively polarized, being responsible for the upward and downward FACs, respectively. On the morning-side, because of the opposite polarization the FACs with reversed directions occur. These FACs correspond to the region 1 and region 2 currents, and they are shown in Fig. 2 where the areas of circles represent the relative FAC inten-

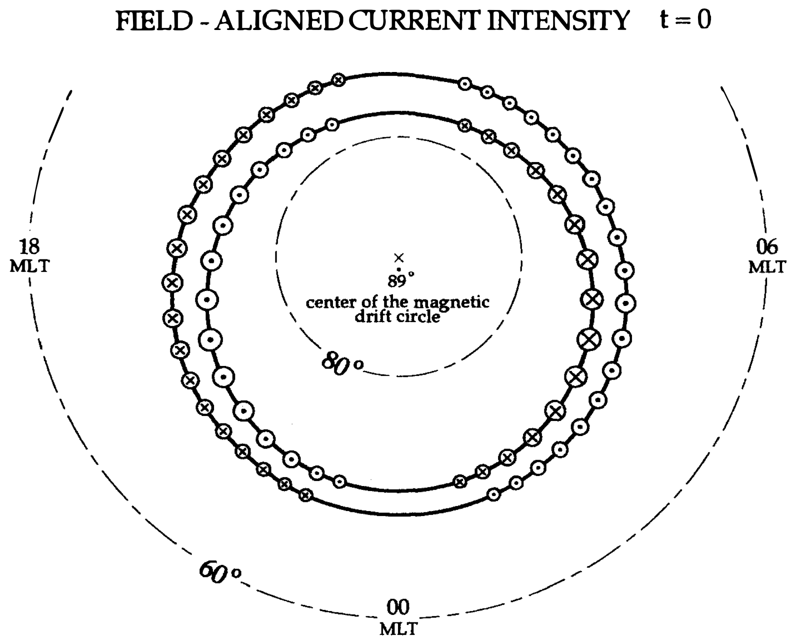

Fig. 2. Initial state in run 1. Distribution of FACs produced on the HPT shown in Fig. 1. A circle with cross or dot inside it is for downward or upward (i.e., toward or away from the ionosphere) FAC, respectively. The areas of circles represent the relative FAC intensity.

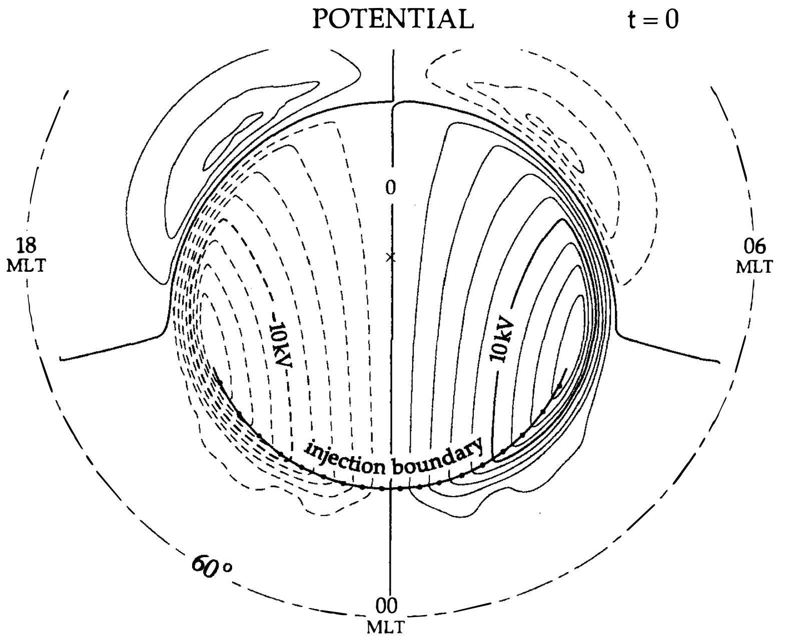

Fig. 3. Initial state in run 1. Electric potential calculated from the Pedersen coupling with the FACs shown in Fig. 2. Solid and dashed contours are for positive and negative potentials, respectively, and the contour interval is 2 kV. The injection boundary (i.e., a part of the open-closed boundary where the inward (toward lower latitude) flow occurs) is also indicated by the line with dots on it.

sity (*i.e.*, latitudinal integration of the current density). Figure 3 shows the electric potential calculated from the Pedersen coupling with the FACs (see assumption 6).

The simulation results of the first run (*i.e.*, run 1) are shown in Figs. 4–7. Figures 4a and 4b show the equicontours of the HPT density n_i and its latitudinal profile at 20 MLT, respectively, when 34 min elapsed. Figure 5 shows the FAC pattern at the same time. Figure 6a shows the corresponding (unmodified) potential, and Fig. 6b shows that at the time of 68 min. Figure 7 shows the temporal variation of the total potential drop. (In Fig. 4b, there is a small amount of the HPT plasma just outside the closed region. The amount of this particle population depends on the processes of outward diffusion and escape of particles: basically, a particle leaving the closed region takes some time to escape, along the (open) field lines, away from the terrestrial region. Taking this fact into account, in the actual simulations (assumption 9) the weight of

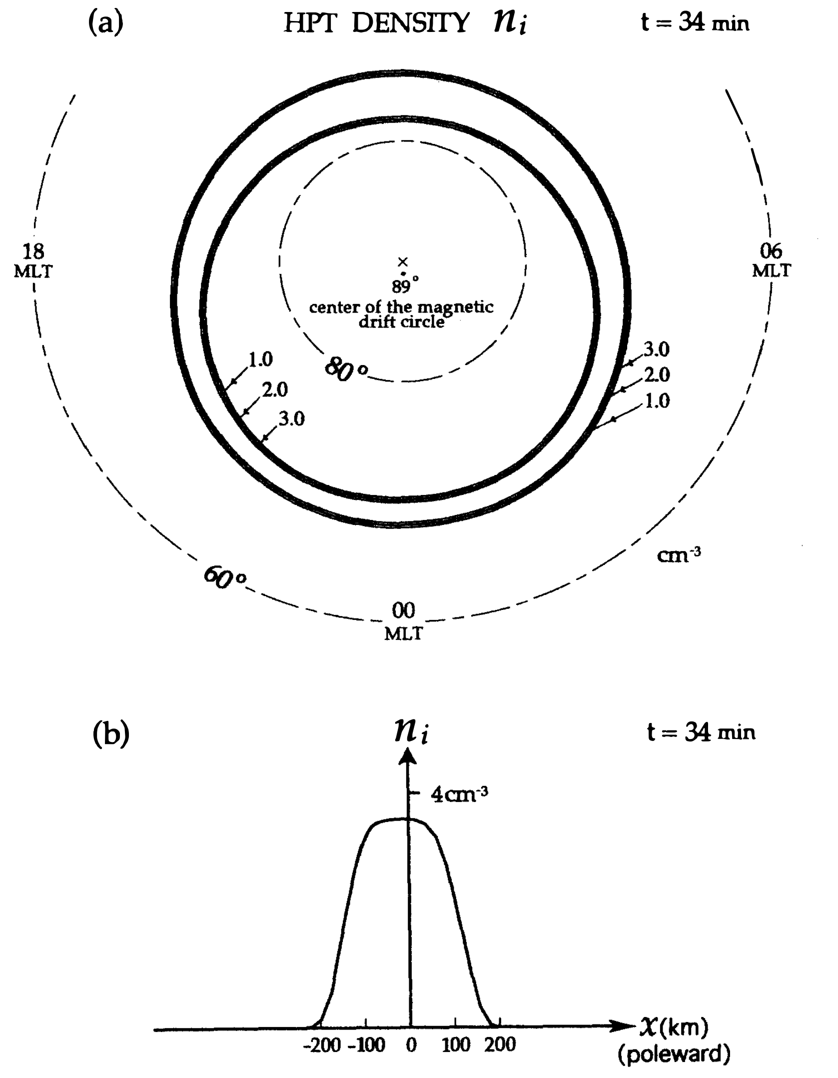

Fig. 4. Results of run 1. (a) Equicontours of the HPT density n_i, and (b) its latitudinal profile at 20 MLT, when 34 min elapsed.

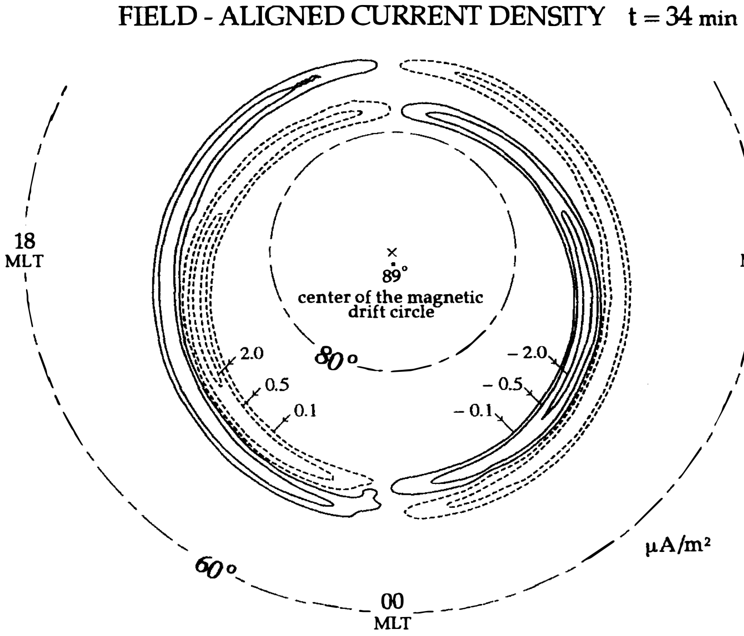

Fig. 5. *Results of run 1. FAC distribution at 34 min. Broken-line equicontours are for upward FAC density $J_{\parallel i}$ (>0) at the ionospheric height, and full-line contours are for downward FAC density $J_{\parallel i}$ (<0). (To facilitate the calculation of FAC densities we assume two distributions of protons and electrons which are displaced, from the HPT particle distribution, by an azimuthal distance greater than that in the actual charge separation. Subsequently we reduce the amount of (separated) charges to give a correct level of the FAC density. This procedure makes the FAC region wider in latitude, compared with that to be ideally identified, but it does not affect the current intensity.)*

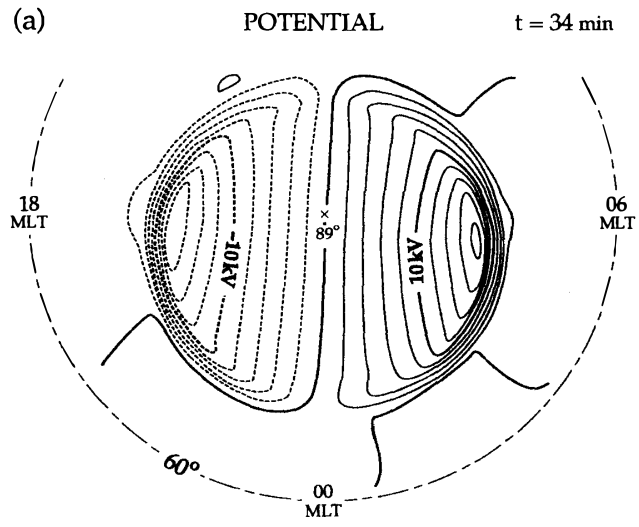

Fig. 6. *Results of run 1. Potential distributions at 34 min (in (a)) and 68 min (in (b)). Same format as Fig. 3.*

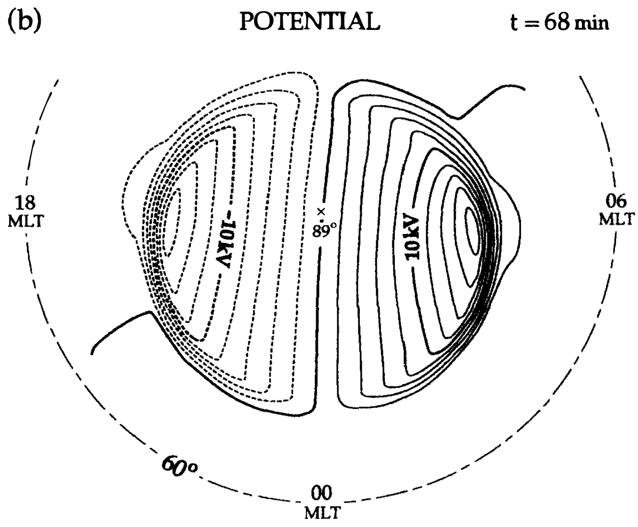

Fig. 6. (Continued).

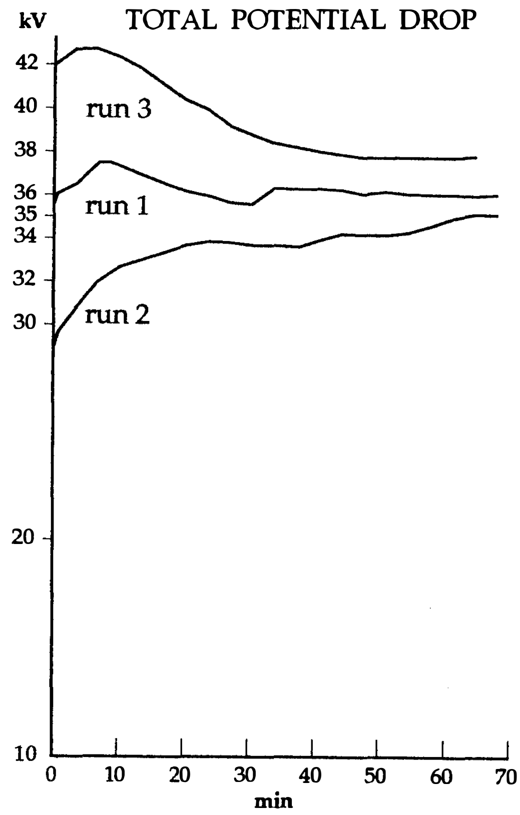

Fig. 7. Temporal variations of total potential drops for runs 1–3.

a particle decreases with time when it lies in the open region, and the time constant for the weight decay is taken to be 5 min (see YAMAMOTO *et al.*, 1997a).

As is seen from Figs. 6 and 7, after a few tens of minutes, the potential profile (the FAC intensity as well) does not significantly change with time, which implies a quasi-steady formation of the HPT as well as the paired region 1/region 2 FAC system. In our model it is assumed that the maintenance of the HPT and the associated current system depends, in energy, on the nonadiabatic acceleration of particles just injected from the (nightside) open-closed boundary. The nonadiabatic particle acceleration is likely to be realized in the magnetic reconnection, which has been thought to be a powerful energy converter transforming magnetic energy into plasma kinetic energy (e.g., SATO *et al.*, 1984). Another interesting feature is the "self-preserving" nature of the HPT: the HPT sets up the $E \times B$ flows by polarizing itself, admitting fresh (energized) particles (from its poleward boundary in the midnight sector) and letting them pass through its main body. Figuratively speaking, the HPT swallows energy/matter from the mouth, absorbs it into the body, and finally excretes. Notably, this operation is possible by the action of the HPT dynamo, namely by converting particle kinetic energy into electrical energy for the FAC system. Finally note that owing to the combined effect of the anomalous cross-field diffusion and the escape to interplanetary space, the latitudinal n_i-profile of the HPT is naturally developed from the rectangular (trapezoidal) shape initially assumed (in Fig. 1b) into a bell shape (in Fig. 4b). On the thus created slope of $\partial N/\partial x < 0$, *i.e.*, the poleward side of the HPT, the region 1 FACs are generated. (Precisely speaking, in the midnight sector where the $E \times B$ flow on the injection boundary has a significant inward component, the n_i-profile is different from the simple bell shape as in Fig. 4b; namely, the density peak occurs relatively near the injection boundary, probably due to contribution from steadily injected particles. A possible fine structure closely associated with the particle injection will be studied in the future by using an advanced simulation model with spatial resolution even higher than that currently used.)

Additional simulation runs are performed to see how the HPT/FAC system evolves from different initial conditions. Specifically, in runs 2 and 3 the centers of circles delineating the equatorward boundary of the initial HPT are positioned at latitudes lower and higher than that in run 1, respectively, and the other conditions are the same

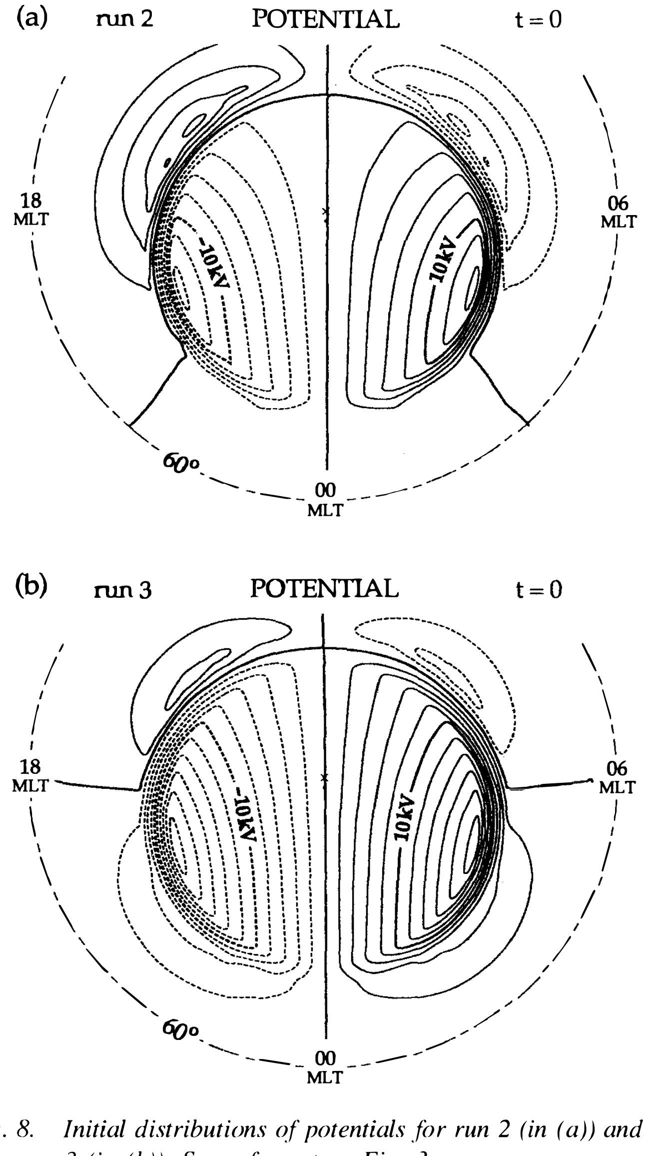

Fig. 8. Initial distributions of potentials for run 2 (in (a)) and run 3 (in (b)). Same format as Fig. 3.

as in run 1. These two conditions physically mean that the equatorward boundaries are subject to stronger and weaker convection-distortions. As a consequence, initially the region 2 FACs in runs 2 and 3 are stronger and weaker, in intensity, compared with that in run 1, and accordingly the total potential drops are smaller and larger, respectively. The initial potential profiles are shown in Figs. 8a and 8b. Temporal variations of the total potential drops in these runs are shown in Fig. 7. An interesting finding here is that as the time proceeds, the potential drop tends to approach a certain asymptotic value, regardless of the degree of the initial distortion of the HPT equatorward boundary. This fact suggests that the HPT evolves into a certain asymptotic configuration which might be determined by boundary conditions and plasma parameters. (Further investigation of such an asymptotic state of the HPT, if any, will be our future work.)

4. Conclusions

By using the two-dimensional simulation model for electrostatic magnetosphere-iono-sphere coupling, we have demonstrated the quasi-steady production of the HPT and simultaneous generation of the paired region 1 and region 2 FACs. For creation and maintenance of this HPT/FAC system, the following processes in the magnetosphere are important: 1) The open-closed boundary is distorted by the two-cell convection. 2) Particles incident on the tail plasma sheet are nonadiabatically accelerated and subsequently they are adiabatically energized. 3) Particles escape, along the open field lines, to the interplanetary space. 4) Particles are subject to the anomalous cross-field diffusion.

Acknowledgments

The work of T. YAMAMOTO was supported in part by the Ministry of Education, Japan, grant 07804029 as well as the joint research programs of Radio Atmospheric Science Center, Kyoto University, Uji, Kyoto and the Institute of Space and Astronautical Science, Sagamihara, Kanagawa.

References

AXFORD, W. I. and HINES, C. O. (1961): A unifying theory of high-latitude geophysical phenomena and geomagnetic storms. Can. J. Phys., **39**, 1433–1464.

DUNGEY, J. W. (1961): Interplanetary field and the auroral zones. Phys. Rev. Lett., **6**, 47–48.

GUSTAFSSON, G. (1970): A revised corrected geomagnetic coordinate system. Ark. Geofys., **5**, 595–617.

HAKURA, Y. (1965): Tables and maps of geomagnetic coordinates corrected by the higher order spherical harmonic terms. Rep. Ionos. Space Res. Jpn., **19**, 121–133.

HRUŠKA, A. (1986): Field-aligned currents in the earth plasma sheet. J. Geophys. Res., **91**, 371–374.

HULTQVIST, B. (1958a): The spherical harmonic development of the geomagnetic field, epoch 1945, transformed into rectangular geomagnetic coordinate systems. Ark. Geofys., **3**, 53–61.

HULTQVIST, B. (1958b): The geomagnetic field lines in higher approximation. Ark. Geofys., **3**, 63–77.

IIJIMA, T. and POTEMRA, T. A. (1976): The amplitude distribution of field-aligned currents at northern high latitudes observed by Traid. J. Geophys. Res., **81**, 2165–2174.

IIJIMA, T. and POTEMRA, T. A. (1978): Large-scale characteristics of field-aligned currents associated with substorms. J. Geophys. Res., **83**, 599–615.

IIJIMA, T., WATANABE, M., POTEMRA, T. A., ZANETTI, L.J. and RICH, F.J. (1991): The relationship between ion and electron precipitation patterns and field-aligned current systems during a substorm. Magnetospheric Substorms, ed. by J. R. KAN *et al.* Washington, D. C., Am. Geophys. Union, 97–110 (Geophys. Mono. Ser., 64).

LEE, W. W. and OKUDA, H. (1978): A simulation model for studying low frequency microinstabilities. J. Comput. Phys., **26**, 139–152.

LYONS, L. R. and SPEISER, T.W. (1982): Evidence for current sheet acceleration in the geomagnetic tail. J. Geophys. Res., **87**, 2276–2286.

MCDIARMID, I. B., BARROWS, J. R. and BUDZINSKI, E. E. (1975): Average characteristics of magnetospheric electrons (150 eV to 200 keV) at 1400 km. J. Geophys. Res., **80**, 73–79.

MCILWAIN, C. E. (1961): Coordinates for mapping the distribution of magnetically trapped particles. J. Geophys. Res., **66**, 3681–3691.

MENG, C.-I., HOLZWORTH, R. H. and AKASOFU, S.-I. (1977): Auroral circle—Delineating the poleward boundary of the quiet auroral belt. J. Geophys. Res., **82**, 164–172.

OKUDA, H. (1985): Introduction to particle simulation models and other application to electrostatic plasma waves in space. Computer Simulation of Space Plasmas, ed. by H. MATSUMOTO and T. SATO. Tokyo, Terra Sci. Publ., 3–41.

SAITO, Y., MUKAI, T., HIRAHARA, M., MACHIDA, S. and KAYA, N. (1992): Distribution function of precipitating ion beams with velocity dispersion observed near the poleward edge of the nightside auroral oval. Geophys. Res. Lett., **19**, 2155–2158.

SATO, T., MATSUMOTO, H. and NAGAI, K. (1982): Particle acceleration in time-developing magnetic reconnection process. J. Geophys. Res., **87**, 6089–6097.

SATO, T., WALKER R. J. and ASHOUR-ABDALLA, M. (1984): Driven magnetic reconnection in three dimensions: Energy conversion and field-aligned current generation. J. Geophys. Res., **89**, 9761–9769.

SISCOE, G. L. and MAYNARD, N. C. (1991): Distributed two-dimensional region 1 and region 2 currents: Model results and data comparisons. J. Geophys. Res., **96**, 21071–21085.

SONNERUP, B. U. Ö. (1980): Theory of the low-latitude boundary layer. J. Geophys. Res., **85**, 2017–2026.

WATANABE, M. and IIJIMA, T. (1993): Substorm growth phase on the magnetotail. J. Geophys. Res., **98**, 17299–17316.

YAMAMOTO, T. and OZAKI, M. (1993): A theory of current generator in the magneto-sphere-ionosphere coupling. Proc. NIPR Symp. Upper Atmos. Phys., **6**, 62–69.

YAMAMOTO, T., MAKITA, K., OZAKI, M. and MENG, C.-I. (1993): A particle simulation of auroral omega bands and torch-like structures. J. Geomagn. Geoelectr., **45**, 619–648.

YAMAMOTO, T., INOUE, S., NISHITANI, N., OZAKI, M. and MENG, C.-I. (1996): A theory for generation of the paired region 1 and region 2 field-aligned currents. J. Geophys. Res., **101**, 27199–27222.

YAMAMOTO, T., INOUE, S. and MENG, C.-I. (1997a): Numerical study on dynamics and polarization of the hot plasma torus in the magnetosphere: Cause of generation of the paired region 1 and region 2 field-aligned currents. J. Geomagn. Geoelectr., **49**, 879–922.

YAMAMOTO, T., INOUE, S. and MENG, C.-I. (1997b): Effect of anomalous cross-field diffusion on the field-aligned current generation. J. Geomagn. Geoelectr., **49**, 923–945.

YAMAMOTO, T., INOUE, S., NISHITANI, N. and MENG, C.-I. (1997c): Interchange stability of the hot plasma torus in the terrestrial magnetosphere. submitted to Phys. Plasmas.

YAMAMOTO, T., INOUE, S. and MENG, C.-I. (1997d): Formation of auroral omega bands in the paired region 1 and region 2 field-aligned current system. J. Geophys. Res., **102**, 2531–2544.

(Received March 11, 1997; Revised manuscript accepted June 20, 1997)